Research Square

Preprints are preliminary reports that have not undergone peer review.
They should not be considered conclusive, used to inform clinical practice,
or referenced by the media as validated information.

Identification and Exploration of Serine Peptidase Inhibitor Kazal Type 1 (SPINK1) as a Potential Biomarker Correlated with the Progression of Non-Small Cell Lung Cancer

Xinxin Zhang
Shandong University Qilu Hospital(Qingdao) https://orcid.org/0000-0001-7252-3642
Rongshuang Ai
Chongqing Medical University
Zhiqiang Ding
Chongqing Institute of Engineering
Zimeng Wang
Chongqing City Hospital of Traditional Chinese Medicine
Qian He
Chongqing Medical University
Yilin Dong
Chongqing Medical University
Yiting Zhu
Chongqing Medical University
Wenzhong Ouyang
Chongqing Qiujing High School
Yujuan He (heyujuan@cqmu.edu.cn)
Chongqing Medical University https://orcid.org/0000-0002-3349-8082

Primary research

Keywords: SPINK1, NSCLC, bioinformatics, proliferation, signaling pathway

Posted Date: March 24th, 2020

DOI: https://doi.org/10.21203/rs.3.rs-18387/v1

License: This work is licensed under a Creative Commons Attribution 4.0 International License.
Read Full License

Abstract

Background Lung cancer is one of the most common malignancies worldwide and is the leading cause of cancer-related death. Approximately 85% of lung cancer patients represent a group of histological subtypes collectively known as non-small cell lung cancer (NSCLC).

Methods To explore the molecular mechanisms underlying tumorigenesis and progression of NSCLC, mRNA expression profiles were downloaded from GEO database (GSE19804, GSE18842, GSE27262, and GSE43458) and differentially expressed genes (DEGs) in NSCLC tissues were analyzed by GEO2R. DEGs in NSCLC tissues were further analysed in TCGA (The Cancer Genome Atlas), GTEx (The Genotype-Tissue Expression Project) and IST (In Silico Transcriptomics) online databases. Serum of NSCLC patients and normal controls were collected and serum concentration of SPINK1 were analysed by ELISA. mRNA and protein expression levels of SPINK1 were analysed by qRT-PCR and western assays. siRNA targeting SPINK1 and normal controls were used for the silence of SPINK1 and GAPDH. CCK-8 assays were employed for cell proliferation detection. Flow cytometric analysis and western blot assays were conducted to assess cell cycle distribution and apoptosis. Western blot assays were performed for the evaluation of cell autophagy and signaling pathways.

Results Among these DEGs, SPINK1 was distinctively up-regulated in NSCLC tissues, which was further validated in TCGA, GTEx and IST databases. Furthermore, serum SPINK1 concentration notably increased in NSCLC patients compared with normal controls. Besides, both mRNA and protein expression levels of SPINK1 significantly increased in human NSCLC cell lines A549 and H1299 compared with normal human bronchial epithelial cell line HBE. Silence of SPINK1 significantly inhibited proliferation of NSCLC cell lines, and exogenous addition of rhSPINK1 partially rescued proliferation suppressed by endogenous knockdown of SPINK1. Mechanistically, silence of SPINK1 could inhibit MEK/ERK signaling pathway, while rhSPINK1 could activate MEK/ERK signaling pathway and then promote proliferation of NSCLC cell lines. In addition, silence of SPINK1 also could activate cell autophagy and apoptosis.

Conclusions Overall, our results suggested that SPINK1 may be a potential biomarker correlated with the progression of NSCLC.

Background

Lung cancer is one of the most common malignancies worldwide as well as the leading cause of cancer-related death (1). Approximately 85% of patients represent a group of histological subtypes collectively known as non-small cell lung cancer (NSCLC), mainly including lung adenocarcinoma (LUAD), lung squamous cell carcinoma (LUSC) and large cell carcinoma (2, 3). Over the past decades, massive efforts have been made for the early diagnosis and treatment of NSCLC (4–6), while the 5-year survival rate for NSCLC is still lower than 17% because of its complicated gene and cell heterogeneities(7). Therefore, it is urgent to uncover the molecular mechanism underlying tumorigenesis and identify new biomarkers related to the progression of NSCLC.

Nowadays, high throughput microarray platforms and sequencing technology have emerged as promising and practical tools for identification of differentially expressed genes (DEGs) in multiple human diseases especially in cancers (8). Gene Expression Omnibus (GEO), the Cancer Genome Atlas (TCGA), the Genotype-Tissue Expression Project (GTEx) and In Silico Transcriptomics (IST) online databases are the most in-demand international public databases for integrated bioinformatic analysis of massive genes in a large sample (9–11). Recently, many DEGs in tumor tissues such as microRNA-17, EZH2, CEP55 and so on were identified by integrated bioinformatic analysis (8, 12).

SPINK1, Serine peptidase inhibitor Kazal type 1, also known as pancreatic secretory trypsin inhibitor (PSTI) and tumor-associated trypsin inhibitor (TATI), is a trypsin inhibitor that was originally isolated from bovine pancreatic tissues (13,14) and later was purified from the urine of patients with ovarian cancer (15). SPINK1 is expressed in multiple tissues and exerts diverse physiological and pathophysiological functions during the process of development and multiple diseases(16–18). Besides, significantly elevated SPINK1 in serum is detected in patients with acute pancreatitis (19). Intriguingly, growing evidence suggested that SPINK1 served as a growth factor playing a role in cancer. Elevated serum SPINK1 was detected and regarded as an independent prognostic factor in several cancers, including renal cancer (20), bladder transitional cell carcinoma (21), metastatic breast cancer (22), hepatocellular carcinoma (23) and ovarian cancer (24, 25). However, the relationship between serum SPINK1 level and the prognosis of patients with colorectal cancer remains controversial (26, 27). In in vitro assays, accumulating evidence confirmed that SPINK1 could promote cell proliferation (28), migration (29), cell cycle distribution (28) and therapeutic resistance (30) while preventing cell apoptosis (31, 32, 33). Mechanically, previous studies suggested that SPINK1 accelerated the progression of malignance mainly through interaction with EGFR thereby activating downstream signaling pathways such as MAPK/ERK, P38, and PI3K/AKT (28, 33). However, the influence and underlying mechanisms of SPINK1 in the progression of NSCLC have not hitherto been clarified clearly.

In this study, we screened 144 DEGs in NSCLC tissues by an integrated bioinformatic analysis and identified SPINK1 as a potential biomarker related to the progression of NSCLC. We demonstrated that SPINK1 significantly inhibited proliferation of NSCLC cell lines partly through MEK/ERK signaling pathway, as well as affected cell cycle distribution, autophagy and apoptosis

Materials And Methods

Microarray datasets and online tools used for integrated bioinformatic analysis. Four human NSCLC mRNA expression datasets were downloaded from the Gene Expression Omnibus database (GEO, https://www.ncbi.nlm.nih.gov/geo/). Detail information of samples was shown as follows: GSE19804: tumor (60 cases) and adjacent normal lung tissue specimens (60 cases) obtained from nonsmoking female non-small cell lung carcinoma (NSCLC) patients in Taiwan. GSE18842: NSCLC samples (46 cases) and control tissues (45 cases). GSE27262: tumor and adjacent normal tissue pairs from 25 stage I lung adenocarcinoma patients. GSE43458: never-smoker adenocarcinomas (40 cases) and never-smoker controls (30 cases). The microarray data of GSE19804, GSE18842, GSE27262 was based on Affymetrix

Human Genome U133 Plus 2.0. Data of GSE43458 was based on Affymetrix Human Gene 1.0 ST Array. GEO2R was used to identify DEGs between NSCLC tissues and normal samples. Heat maps were drew by HemI. Venn Diagram showed the intersections of DEGs obtained from different datasets (http://bioinfogp.cnb.csic.es/tools/venny/index.html/). Gene expression profiles among 59 normal lung tissue cases and 533 NSCLC samples were downloaded from The Cancer Genome Atlas (TCGA, https://cancergenome.nih.gov/). Data from GTEx (The Genotype-Tissue Expression Project) were obtained using online Gene Expression Profiling Interactive Analysis (GEPIA, http://gepia.cancer-pku.cn/). mRNA expression levels of SPINK1 in normal and tumor tissues among different cancers were analysed by In Silico Transcriptomics online databases (IST, http://ist.medisapiens.com/). Functional enrichment analysis of the DEGs, including Gene Ontology (GO) and Kyoto Encyclopedia of Genes and Genomes (KEGG) pathway enrichment analyses were accomplished by an online tool (http://www.funrich.org/).

ELISA. Serum of 20 normal controls, 38 NSCLC patients, and 11 pleural effusion of NSCLC patients in Chongqing Hospital of Traditional Chinese Medicine during 2018.02-2018.06 were collected. This study was conducted in accordance with the principles of good clinical practice and apporved by the Ethics Committee of Chongqing Medical University. SPINK1 concentrations were detected by ELISA (BOSTER,EK1241) according to the reference manual.

Cell culture. Normal human bronchial epithelial cell line HBE, human non-small cell lung cancer cell line H1299, human squamous cell carcinoma cell line SK-MES-1 and human large cell lung cancer cell line H460 were maintained in complete culture medium (RPMI 1640 with 10% fetal bovine serum (FBS), 100 units/mL penicillin, and 100 μg/mL streptomycin). Human non-small cell lung cancer cell line A549 were routinely cultured with F-12K medium (10% FBS). All cell lines were grown at 37 °C in an atmosphere with 5% CO_2. Cell number were determined using a Neubauer hemocytometer.

RNA interference and exogenous addition of SPINK1. Small interfering RNAs targeting SPINK1 and the negative control were obtained from TSINGKE (Shanghai, China). The target sequences were as follows:

si-NC: 5′-TTCTCCGAACGTGTCACGT-3′;

si-SPINK1-1: 5′-GCCAGACUUCUAUCCUCAUTT-3′. Cells were seeded in corresponding culture plates and cultured with antibiotics-free medium overnight. Next day the growth medium was removed and cells were transfected with siRNAs (50 nM) using Lipofectamine 2000 (Invitrogen) according to the manufacturer's protocol when cell density was increased to 50–70%. rhSPINK1 was purchased from R&D (#7496-PI-010).

RNA extraction and quantitative real-time PCR. Total RNA was extracted using IsoPlus reagent (Takara Bio, Japan) following the manufacturer’s protocol and then 1 μg RNA was reverse transcribed with random primers using a PrimeScript™ RT reagent Kit (Takara Bio, Japan). cDNA was amplified using SYBR green master mix (TaKaRa Bio, Japan) on an ABI 7500 Fast RealTime PCR system

(Sigma-Aldrich, St. Louis, MO, USA). GAPDH was amplified as an internal reference. Primers were as follows:

SPINK1-F, TGTGTGT GGGACTGATGGAA;

SPINK1-R,AGGCCCAGATTTTTGAATGA;

GAPDH-F,ACGGCAAATTCAACGGCACAGTCA; GAPDH-R,TGGGGGCATCGGCAGAAGG.

Viability assay. The Cell Counting Kit-8 (CCK-8) assay was employed to quantify the vitality of cells. Cells were seeded into 96-well plates at a concentration of 2×10^4 cells/mL and cultured with antibiotics-free medium overnight. The next day cells were transfected with siRNA (50 nM). Then 10 μL CCK8 reagent (Solarbio, China) were added to each well at 0, 24, 48, and 72 hours respectively. Cells were incubated for 2.5 hours in the dark at 37 °C. The absorbance at 450 nm was measured by Biotek reader (ELx800, USA).

Growth curve. 2×10^4 A549 cells were seeded into 24-well plates and transfected with si-NC and si-SPINK1-1 (50 nM). Total numbers of cells were determined by trypsinization and cell counting using a Neubauer hemocytometer at 0 h, 48 h,72 h and 96 h post transfection.

Flow cytometric analysis of cell cycle distribution. 3×10^5 cells were seeded in six-well plates and treated with siRNAs (50 nM) as described perviously. Cells were collected by trypsinization at 48 hours after transfection and washed with cold PBS followed by fixation in 70% ethanol for 12 hours at -20℃. After washing with PBS for three times, cells were incubated in PBS with 0.1 mg/mL RNase (Solarbio, China) at 37 °C for 30 minutes. Then, cells were stained with PI (25 μg/ml, Sigma, USA) in the dark for 10 minutes. The stained nuclei were counted by flow cytometry and the cell cycle profile was analysed by the FlowJo software.

Flow cytometric analysis of apoptosis. 1.5×10^5 cells were seeded in 12-well plates and transfected with corresponding siRNAs (50 nM) as described previously. Change culture medium with serum-free culture medium supplemented with 0.3% BSA 24 h post transfection. Total cells were collected by trypsinization at 60 hours after transinfection and washed with cold PBS for twice. Collected cells were double stained with FITC-Annexin V and PI using FITC Annexin V Apoptosis Detection Kit (BD Biosciences) according to the protocols. The stained cells were analyzed by BD FACSJazz flow cytometer (BD Biosciences), and the data was analyzed using Cell Quest software (BD Biosciences).

Western blot. Total protein was extracted using radioimmunoprecipitation assay (RIPA) lysis buffer (Beyotime, China) supplemented with 1 mM PMSF (Beyotime, China) and phosphatase inhibitor cocktail A and B (Beyotime, China), quantified using the Enhanced BCA Protein Assay Kit (Beyotime, China), and denatured by boiling with SDS-PAGE Sample Loading Buffer (Beyotime, China) for 10 minutes. Protein samples (40 μg) were separated by 12% SDS-PAGE, and transferred onto polyvinylidene difluoride (PVDF, 0.20 μm) membranes (Millipore, Bedford, MA). The membranes were blocked with 5% bovine serum albumin in Tris-buffered saline containing 0.1% Tween-20 at 37℃ for 2 h and then incubated with

primary antibodies at 4℃ overnight. The primary antibodies were as follows : SPINK1 (sc-37440, 1:500, Santa Cruz, CA), GAPDH (#5174, 1:8000, CST, USA); p-MEK1/2 (#2338, 1:1000, CST, USA); MEK1/2 (#8727, 1:1000, CST, USA); pERK (#4370, 1:1000, CST, USA); Erk1/2 (#9102, 1:1000, CST, USA); pPI3K (#4228, 1:500, CST, USA); PI3K (#4292, 1:800, CST, USA); pAkt (Ser473)(#4060, 1:500, CST, USA); Akt (#4691, 1:800, CST, USA); LC3 (#12741, 1:1000, CST, USA); P62 (#3912, 1:1000, CST, USA); ATG7 (#8558, 1:800, CST, USA); CDK4 (#12790, 1:1000, CST, USA); Bax (#5023, 1:1000, CST, USA); BCL2 (#196495, Abcam, USA). The membranes were washed for 30 minutes with TBST and subsequently incubated with the corresponding secondary antibody (#656120, HRP goat anti rabbit, 1:10000, Invitrogen; #A32723, HRP goat anti mouse, 1:10000, Invitrogen) for 1 h at 37℃. Membranes were then washed another three times for 30 minutes with TBST. Protein bands were visualized using Super Signal electrochemiluminescence (#34580, Thermo Scientific) and quantitated with image Pro Plus 6.0, and the data were normalized to GAPDH.

Statistical analysis. Data represent three independent experiments and are presented as mean ± SD (n = 3). GraphPad Prism software (version 5.01) was applied for statistical analysis. Unpaired t tests were used for data with a normal distribution. Differences with $p < 0.05$ were considered statistically significant.*$P < 0.05$; **$P < 0.01$; ***$P < 0.001$.

Results

1. Convergence of DEGs in NSCLC tissues via integrated bioinformatic analysis

To identify novel biomarkers related to the pathogenesis and progression of NSCLC, mRNA expression profiles from cancerous and normal lung tissues were downloaded from GEO datasets (GSE19804, GSE18842, GSE27262, and GSE43458) and analyzed by GEO2R respectively. p value < 0.05 and | LogFC | >1.5 were applied as screening criteria. DEGs identified from the four datasets were as follows: GSE19804: with 129 up-regulated and 382 down-regulated genes; GSE18842: with 634 up-regulated and 902 down-regulated genes; GSE27262: with 357 up-regulated and 695 down-regulated genes; GSE43458: with 54 up-regulated and 178 down-regulated genes（data not shown）. mRNA profiles were downloaded from GSE19804 dataset and analyzed with GEO2R. Heapmaps showed 41 up-regulated genes (LogFc>2) (Fig. 1a) and 64 down-regulated genes (|LogFC|>2.5) (Fig. 1b).Venn Diagram demonstrated the intersections of DEGs obtained from the four datasets, including 23 commonly up-regulated genes (Fig.1c) and 121 commonly down-regulated genes (Fig.1d). These 144 DEGs were further subjected to functional annotation. Results showed that these DEGs were mainly expressed in the plasma membrane, cytoplasm, extracellular and nucleus of cells (Fig. 1e), acting as cell adhesion molecules, metallopeptidases and receptors (Fig. 1f) involved in a variety of biological processes such as cell communication, signal transduction, growth supporting, and metabolism process (Fig. 1g). In addition, these genes are also abnormally expressed in breast cancer, liver cancer, kidney cancer, head and neck tumors (Fig. 1h), indicating that these genes are universally disordered in various human tumors and may lead to enhanced activities of proliferation, invasion and immunologic tolerance of cancer cells.

2. SPINK1 increased in NSCLC tissues, serum and cell lines

Among above 23 up-regulated DEGs, SPINK1 is one of the most overexpressed EDGs on GEO (Fig.1a), TCGA (Fig.2a), GTEx (Fig.2b) and In Silico Transcriptomics (IST) (Fig.2c) online databases. Given that SPINK1 is a secretory protein and the concentration of serum SPINK1 is enhanced in several cancers, serum of 20 normal controls and 38 NSCLC patients, and pleural effusion of 11 NSCLC patients were collected to detect the SPINK1 concentration by ELISA. As shown in Fig.2d, serum SPINK1 in NSCLC patients was significantly higher than normal controls (1092.9pg/mL vs 644.5pg/mL, $p<0.01$). Furthermore, the concentration of SPINK1 in pleural effusion was higher than that in serum of NSCLC patients (1928.8pg/mL vs 1092.9pg/mL, $p<0.01$). Subsequently, expression levels of SPINK1 in HBE, A549, H1299, SK-MES-1, and H460 were assessed by qRT-PCR and western blot. Results suggested that expression levels of SPINK1 in A549 and H1299 substantially increased compared with HBE (Fig.2e, Fig.2f). Besides, SPINK1 presented higher expression in A549 and H1299 compared with SK-MES-1 and H460 (Fig.2f).

3. SPINK1 promotes proliferation of NSCLC cells

To investigate the effect of SPINK1 on the proliferation of NSCLC cell lines, siRNAs targeting SPINK1 were transfected into NSCLC cell lines. qRT-PCR (Fig.3a, S Fig.1a) and western blot (Fig.3b, S Fig.1b) results confirmed successful knockdown of SPINK1 in A549 and H1299 cell lines respectively. CCK8 assay and growth curve were applied to detect the vitality of cells and results indicated that silence of SPINK1 significantly inhibited cell proliferation of A549 and H1299 (Fig.3c, Fig.3d, S Fig.1c). Given that SPINK1 is a secreted soluble protein, we speculated that exogenous addition of rhSPINK1 could stimulate the proliferation of H460 with relatively low SPINK1 expression. CCK8 assay results confirmed that rhSPINK1(1ng/mL) promoted the proliferation of H460 (Fig.3e). Moreover, addition of exogenous rhSPINK1(5ng/mL) could rescue cell vitality of A549 and H1299 after transfection with si-SPINK1-1 (Fig.3f, S Fig.1d). Apart from that, silencing SPINK1 in A549 and H1299 caused cell cycle arrest, with strikingly increased proportion of cells in G_1-phase and decreased proportion of cells in S-phase (Fig. 4a, S Fig. 2a). Consistently, silencing SPINK1 decreased the expression of cell cycle checkpoint protein CDK4 in A549 (Fig.4b) and H1299 (S Fig.2b). Above results validated that SPINK1 promotes proliferation of NSCLC cell lines.

4. Silence of SPINK1 activates autophagy and apoptosis of NSCLC cells

Both autophagy and apoptosis are vital process during progression of development and oncogenesis. As shown in Fig. 5a, silence of SPINK1 in A549 activated autophagy characterized by increased expression of Beclin-1 and ATG7, decreased P62 and increased ratio of LC3 II/LC3I. Consistently, knockdown of SPINK1 in H1299 induced excessive autophagy (S Fig. 3a). Meanwhile, silence of SPINK1 increased expression of pro-apoptosis protein BAX and decreased expression of anti-apoptosis protein BCL-2 (Fig.5b). Consistently, flow cytometry analysis indicated that silence of SPINK1 in A549 and H1299 resulted in cell apoptosis (Fig.5c, S Fig.3b, S Fig.3c).

5. SPINK1 accelerates the proliferation of NSCLC via activation of MEK/ERK signaling pathway

It has been universally accepted that SPINK1 acting as a pro-survival factor accelerated the progression of multiple cancers by interacting with EGFR (25, 28, 29, 38, 53). In order to clarify signaling pathways downstream of EGFR mediating the carcinogenic effect of SPINK1 in NSCLC, the phosphorylation levels of MEK1/2, ERK, PI3K and AKT were assessed by western blot. Results showed that silence of SPINK1 in A549 and H1299 cells decreased the phosphorylation levels of MEK1/2, ERK, PI3K and AKT, and MEK/ERK signaling pathway represented more significant inhibition (Fig. 6a, S Fig. 4a). In addition, WB results demonstrated that rhSPINK1(5ng/mL) could increase the phosphorylation levels of p-ERK, which was inhibited by U0126 (10μM, the specific inhibitor of MEK) (Fig. 6b, S Fig. 4b). Further, CCK8 results showed that rhSPINK1 (5ng/mL) accelerated proliferation of A549 and H1299, which were suppressed by the pretreatment of U0126 (Fig. 6c, S Fig. 4c). Collectively, SPINK1 could promote the proliferation of NSCLC through MEK/ERK signaling pathway.

Discussion

In our present study, mRNA expression profiles were downloaded from GEO, TCGA, GTEx and IST databases and analyzed by integrated bioinformatic analysis. 144 DEGs were identified in NSCLC tissues compared with normal lung tissues. Among these DEGs, SPINK1 attracted our attention, for there are few reports about the effect and mechanism of SPINK1 on the progression of NSCLC up to date.

Numerous studies have shown that SPINK1 plays multiple biological roles under various physiological and pathological conditions. As a serpin typically produced by pancreatic acinar cells, SPINK1 functions to defense against trypsinogen activation in the acini and the pancreatic ducts (34). Serving as an acute phase reactant, SPINK1 is increasingly secreted into blood in a state of stress such as major surgery and serious inflammatory and septic complications (16). Ken-ichi Yamamura et al. reported that SPINK3, the homologous gene of SPINK1 in mouse, may participate in the differentiation and development of mouse embryo (35). In addition, SPINK1 secreted by cancer cells could co-immmunoprecipitate with serine protease granzyme A (GzmA), a cytolytic granule secreted by natural killer cells and cytotoxic T lymphocytes, thereby suppressing GzmA-mediated apoptosis and establishing a tolerance of cancer cells to the immune surveillance system (32). More importantly, SPINK1, as a growth factor, is aberrantly expressed in multiple human cancers such as ovarian cancer (33), prostatic cancer (36), colorectal cancer (37), hepatocellular carcinoma (38) and pulmonary adenocarcinoma (39). Based on big data analysis, we detected a significant increase of SPINK1 expression in NSCLC tissues. Consistently, a recent study reported that tissue SPINK1 is over-expressed in NSCLC patients (40). Additionally, SPINK1 could be detected in serum and act as independent prognostic factor in prostatic cancer (41), hepatocellular carcinoma (42), bladder transitional cell carcinoma (21), colorectal cancer (26) and renal cancer (43). So we speculated that serum SPINK1 might serve as a potential and promising biomarker in NSCLC. In our study, we founded that concentration of SPINK1 in serum of NSCLC patients was higher than normal controls, and concentration of SPINK1 in pleural effusions was even higher than in serum, which may

shed new insight into early body fluid diagnosis of NSCLC. In the following study, we will further explore relationships between serum SPINK1 level and NSCLC stage, metastasis and overall survival of patients.

In our study, we founded that the expression of SPINK1 increased in A549 and H1299 cells compared with HBE, which was consistent with the report that well-differentiated adenocarcinoma tissues express stronger SPINK1 (39). In in vitro experiments, we demonstrated that SPINK1 played a role in cell cycle distribution of NSCLC cell lines. In eukaryotes, DNA replication is limited in S-phase, and chromosome segregation occurs at M-phase. Two gap phases, known as G1 and G2, separate S-phase and M-phase. Multiple cell cycle checkpoints participate in the regulation of cell cycle progression such as cyclin-dependent kinases (CDKs), cyclins and CDKs inhibitors (CKI). CDKs act as engine to drive cell cycle progression (44). Previous reports suggested that during the G1 phase, CDK4/cyclin D and CDK2/cyclin E complexes could phosphorylate Rb, inducing the activation of E2F and the transcription of E2F responsive genes, which are required for G1/S transition (45, 46). In our studies, we indicated that silence of SPINK1 in A549 and H1299 cells resulted in cell cycle arrest, with increased percentage of cells in G_1-Phase and decreased percentage of cells in S-Phase. In addition, western blot assays showed decreased expression of CDK4 in SPINK1 silencing groups. Consistent with our results, Caj Haglund et al. reported that upregulation of SPINK1 in BRL-3A cells could increase cell numbers in S-Phase and G_2/M Phase (28).

Autophagy is a process characterized by engulfing cytoplasmic proteins, complexes or organelles into the autophagosome. Accumulating evidence confirmed that there is a crosstalk between autophagy and apoptosis. In basal state, Beclin-1 binds to BCL-2, an anti-apoptotic protein, and then autophagy and apoptosis are inhibited. A short period (4 h) of nutrient starvation could activate c-Jun N-terminal protein kinase 1 (JNK1), following that BCL-2 was phosphorylated by p-JNK1 and then dissociated with Beclin-1, thereby activating autophagy. During the short period of nutrient starvation, phosphorylated BCL2 binds with pro-apoptotic protein BAX and exerts an anti-apoptotic effect (47, 48). However, BCL-2 is hyperphosphorylated and the BCL-2/Bax complex is disrupted after 16 hours of nutrient starvation, followed by the activation of caspase 3 and the initiation of apoptosis (49). YAMAMURA et al. reported autophagic cell death of pancreatic acinar cells in SPINK3 deficient mice, with increased ratio of LC3 II/LC3 I and increased formation of autophagosome (50). In our study, NSCLC cells were transfected with siRNAs and cultured with incomplete culture medium containing 2% FBS for 48 h. Consistent with these reports, we showed that silence of SPINK1 activated autophagy and apoptosis. To some extent when autophagy is no longer able to matain cell survival, apoptosis will be initiated, with decreased expression of anti-apoptosis protein BCL-2 and increased expression of pro-apoptosis protein BAX. In our models, we speculated that silence of SPINK1 conferred sensitivity to starvation and induced excessive autophagy and apoptosis.

At present, most reports indicated that SPINK1 phosphorylates EGFR and thereby acting the downstream signaling pathways to exert oncogenic effect. MEK/ERK (25, 29 38, 53) p38 (28) and PI3K/AKT (51) signaling pathways were reported as executants downstream of EGFR. In our studies, we validated that silence of SPINK1 decreased the phosphorylation levels of MEK1/2, ERK, PI3K and AKT, while producing

no effect on phosphorylation levels of p38. Notably, compared with PI3K/AKT signaling pathway, more significant decrease of MEK/ERK phosphorylation levels was observed after treatment with rhSPINK1. Further, MEK/ERK signaling pathway and cell proliferation of NSCLC cells were suppressed by higher doses of MEK inhibitor, U0126, indicating that SPINK1 could accelerate progression of NSCLC partially through MEK/ERK signaling pathways.

In summary, our study revealed that silence of SPINK1 in NSCLC cell lines could inhibit cell proliferation, induce cell cycle arrest, and activate cell autophagy and apoptosis. SPINK1 promotes progression of NSCLC partially through MEK/ERK signaling pathway. Our study presented evidence in support of SPINK1 as a potential bio-target in the progression of NSCLC and provides new insight into the underlying mechanism.

Abbreviations

NSCLC
Non-small cell lung cancer
LUAD
Lung adenocarcinoma
LUSC
Lung squamous cell carcinoma
SPINK1
Serine Peptidase Inhibitor Kazal Type 1
DEGs
Differentially expressed genes
GTEx
Genotype-Tissue Expression Project
GEO
Gene Expression Omnibus; https://www.ncbi.nlm.nih.gov/geo/
TCGA
The Cancer Genome Atlas; https://cancergenome.nih.gov/
GEPIS
Gene Expression Profiling Interactive Analysis; http://gepia.cancer-pku.cn/
IST
In Silico Transcriptomics; http://ist.medisapiens.com/
PSTI
Pancreatic secretory trypsin inhibitor
TATI
Tumor-associated trypsin inhibitor
GO
Gene ontology; http://www.funrich.org/
KEGG

Kyoto encyclopedia of genes and genomes; http://www.funrich.org/
CCK-8
The Cell Counting Kit-8

Declarations

Ethics approval and consent to participate

This study was conducted in accordance with the principles of good clinical practice and apporved by the Ethics Committee of Chongqing Medical University.

Consent for publication

Not applicable

Availability of data and materials

The raw data supporting the conclusions of this manuscript will be made available by the authors, without undue reservation, to any qualified researcher.

Competing interests

The authors declare that the research was conducted in the absence of any commercial or financial relationship that could be construed as a potential conflict of interest.

Funding

This study is supported by National Natural Science Foundation grants of China (No. csfc81373151) and Natural Science Foundation Project of CQCSTC (No. cstc2018jcyjAX0257).

Author contributions

XZ and YH conceived of and designed the research. XZ, QH, YLD, YTZ, and RSA performed the experiments and analyzed the data. XZ and YH wrote the manuscript. ZMW and CFJ interpreted the data and corrected the manuscript.

Acknowledgements

We thank Zhiqiang Ding for the correction of the English usage of the manuscript.

References

1. Hong QY, Wu GM, Qian GS,et al. Prevention and management of lung cancer in China. Cancer.2015 Sep 1;121 Suppl 17:3080-8.

2. Xiaohu Zheng, Min Cheng, Binqing Fu, Xiaolei Fan, Qing Wang, Xiaoqing. Targeting LUNX inhibits non-small cell lung cancer growth and metastasis. Cancer Res 2015 Mar 15; 75 (6):1080-90.
3. Molina JR, Yang P, Cassivi SD, Schild SE, Adjei AA. Non-small cell lung cancer: epidemiology, risk factors, treatment, and survivorship. Mayo Clin Proc 2008 May; 83(5): 584-94.
4. Tanvetyanon T, Gray JE, Antonia SJ. PD-1 checkpoint blockade alone or combined PD-1 and CTLA-4 blockade as immunotherapy for lung cancer? Expert Opin Biol Ther 2017 Mar;17(3):305-312.
5. Sheng Z, Zhu X, Sun Y, Zhang Y. The efficacy of anti-PD-1/PD-L1 therapy and its comparison with EGFR-TKIs for advanced non-small-cell lung cancer. Oncotarget 2017 Jun 8;8(34):57826-57835.
6. Herbst RS, Morgensztem D, Boshoff C. The biology and management of non-small cell lung cancer. Nature 2018 Jan 24;553(7689):446-454.
7. Hirsch FR, Scagliotti GV, Mulshine JL, Kwon R, Curran WJ Jr, Wu YL, Paz-Ares L. Lung cancer: current therapies and new targeted treatments. Lancet 2017 Jan 21;389(10066):299-311.
8. Hu G, Lv Q, Yan J, Chen L, Du J, Zhao K, Xu W. MicroRNA-17 as a promising diagnostic biomarker of gastric cancer: an investigation combining TCGA, GEO, meta-analysis, and bioinformatcs. FEBS Open Bio 2018 Aug 30;8(9):1508-1523.
9. Chu YH, Su CW, Hsieh YS, Chen PN, Lin CW, Yang SF. Carbonic Anhydrase III Promotes Cell Migration and Epithelial-Mesenchymal Transition in Oral Squamous Cell Carcinoma.2020 Mar 13;9(3).
10. Lee JS. Exploring cancer genomic data from the cancer genome atlas project. BMB Rep 2016 Nov;49(11):607-611.
11. Gao J, Dai C, Yu X, Yin XB, Zhou F. LncRNA LEF1-AS1 silencing diminishes EZH2 expression to delay hepatocellular carcinoma development by impairing CEBPB-interaction with CDCA7. Cell Cycle.2020 Mar 16:1-14.
12. Li Y, Gu J, Xu F, Zhu Q, Ge D, Lu C. Transcriptomic and functional network features of lung squamous cell carcinoma through integrative analysis of GEO and TCGA data. Sci Rep 2018 Oct 26;8(1):15834.
13. Guo M, Zhou X, Han X, Zhang Y, Jiang L. SPINK1 is a prognosis predicting factor of non-small cell lung cancer and regulates redox homeostasis.Oncol Lett. 2019 Dec;18(6):6899-6908.
14. Kazal LA, Spicer DS, Brahinsky RA. Isolation of a crystalline trypsin inhibitor anticoagulant protein from the pancreas. J AmChemSoc 1948; 70:3034–40.
15. Stenman UH, Huhtala ML, Koistinen R, Seppala M. Immunochemical demonstration of an ovarian cancer-associated urinary peptide. Int J Cancer 1982;30:53–7.
16. Ogawa M. Pancreatic secretory trypsin inhibitor as an acute phase reactant. Clin Biochem 1988 Jan;21(1):19-25.
17. Zhu C, Han H, Li J, Xu L, Liu F, Wu K, Liu X. Hepatitis B Virus X Protein-Induced Serine Protease Inhibitor Kazal Type 1 Is Associated with the Progression of HBV-Related Diseases.Biomed Res Int. 2019 May 22;2019:9321494.

18. Bhatia V, Yadav A, Tiwari R, Nigam S, Goel S, Carskadon S, Gupta N, Goel A, Palanisamy N, Ateeq B. Epigenetic Silencing of miRNA-338-5p and miRNA-421 Drives SPINK1-Positive Prostate Cancer. Clin Cancer Res. 2019 May 1;25(9):2755-2768.

19. Muller N, Sarantitis I, Rouanet M, de Mestier L, Halloran C, Greenhalf W, Férec C, Masson E, Ruszniewski P, Lévy P, Neoptolemos J, Buscail L, Rebours V. Natural history of SPINK1 germline mutation related-pancreatitis. 2019 Oct;48:581-591.

20. Lukkonen A, Lintula S, von Boguslawski K,Carpén O, Ljungberg B, Landberg G, Stenman UH. Tumor-associated trypsin inhibitor in normal and malignant renal tissue and in serum of renal-cell carcinoma patients. Int J Cancer 1999;83:486–90.

21. Kelloniemi E, Rintala E, Finne P, Stenman UH; Finnbladder Group. Tumor-associated trypsin inhibitor as a prognostic factor during follow-up of bladder cancer. Urology 2003 Aug;62(2):249-53.

22. El-mezayen HA, Metwally FM, Darwish H. A novel discriminant score based on tumor-associated trypsin inhibitor for accurate diagnosis of metastasis in patients with breast cancer. Tumour Biol 2014 Mar;35(3):2759-67.

23. Lyytinen I, Lempinen M, Nordin A, Makisalo H, Stenman UH, Isoniemi H. Prognostic significance of tumor-associated trypsin inhibitor (TATI) and human chorionic gonadotropin-beta (hCGbeta) in patients with hepatocellular carcinoma. Scand J Gastroenterol 2013;48:1066–

24. Paju A, Vartiainen J, Haglund C,Itkonen O, von Boguslawski K, Leminen A, Wahlström T, Stenman UH. Expression of trypsinogen-1, trypsinogen-2, and tumor-associated trypsin inhibitor in ovarian cancer: prognostic study on tissue and serum. Clin Cancer Res 2004;10:4761–

25. Venesmaa P, Stenman UH, Forss M, Leminen A, Lehtovirta P, Vartiainen J, Paavonen J. Pre-operative serum level of tumour associated trypsin inhibitor and residual tumour size as prognostic indicators in Stage III epithelial ovarian cancer. Br J Obstet Gynaecol 1998;105:508–11.

26. Gaber A, Nodin B, Hotakainen K, Nilsson E, Stenman UH, Bjartell A, Birgisson H, Jirström K. Increased serum levels of tumour-associated trypsin inhibitor independently predict a poor prognosis in colorectal cancer patients. BMC Cancer 2010;10:498.

27. Koskensalo S1, Louhimo J, Hagström J, Lundin M, Stenman UH, Haglund C. Concomitant tumor expression of EGFR and TATI/SPINK1 associates with better prognosis in colorectal cancer. PLoS One 2013 Oct 25 ; 8(10):e76906.

28. Chang C, Zhao W, Luo Y, Xi L, Chen S, Zhao C, Wang G, Guo J, Xu C. Serine peptidase inhibitor Kazal type I (SPINK1) promotes BRL-3A cell proliferation via p38, ERK, and JNK pathways. Cell Biochem Funct 2017 Aug;35(6):339-348.

29. Marchbank T, Mahmood A, Playford RJ. Pancreatic secretory trypsin inhibitor causes autocrine-mediated migration and invasion in bladder cancer and phosphorylates the EGF receptor, Akt2 and Akt3, and ERK1 and ERK2.Am J Physiol Renal Physiol 2013 Aug 1;305(3):F382-9.

30. Chen F, Long Q, Fu D, Zhu D, Ji Y, Han L, Zhang B, Xu Q, Liu B, Li Y, Wu S, Yang C, Qian M, Xu J, Liu S, Cao L, Chin YE, Lam EW, Coppé JP, Sun Y. Targeting SPINK1 in the

damaged tumour microenvironment alleviates therapeutic resistance. Nat Commun 2018 Oct 17;9(1):4315.

31. Egger L1, Schneider J, Rhême C, Tapernoux M, Häcki J, Borner C. Serine proteases mediate apoptosis-like cell death and phagocytosis under caspase-inhibiting conditions. Cell Death Differ 2003 Oct; 10(10):1188-203.
32. Lu F, Lamontagne J, Sun A, Pinkerton M, Block T, Lu X. Role of the inflammatory protein serine protease inhibitor Kazal in preventing cytolytic granulegranzyme A-mediated apoptosis. Immunology 2011 Dec; 134(4):398-408.
33. Mehner C, Oberg AL, Kalli KR, Nassar A, Hockla A, Pendlebury D, Cichon MA, Goergen KM, Maurer MJ, Goode EL, Keeney GL, Jatoi A, Sahin-Tóth M, Copland JA, Radisky DC, Radisky ES. Serine protease inhibitor Kazal type 1 (SPINK1) drives proliferation and anoikis resistance in a subset of ovarian cancers. Oncotarget 2015 Nov 3;6(34):35737-54.
34. Ohmuraya M, Hirota M, Araki K, Baba H, Yamamura K. Enhanced trypsin activity in pancreatic acinar cells deficient for serine protease inhibitor Kazal type 3. Pancreas 2006;33:104–6.
35. Wang J, Ohmuraya M, Hirota M, Baba H, Zhao G, Takeya M, Araki K, Yamamura K. Expression pattern of serine protease inhibitor Kazal type3 (Spink3) during mouse embryonic development. Histochem Cell Biol 2008 Aug;130(2):387-97.
36. Paju A, Hotakainen K, Cao Y, Laurila T, Gadaleanu V, Hemminki A, Stenman UH, Bjartell A. Increased expression of tumor-associated trypsin inhibitor, TATI, in prostate cancer and in androgen-independent 22Rv1 cells. Eur Urol 2007;52:1670–
37. Higashiyama M, Monden T, Tomita N, Murotani M, Kawasaki Y, Morimoto H, Murata A, Shimano T, Ogawa M, Mori T. Expression of pancreatic secretory trypsin inhibitor (PSTI) in colorectal cancer. Br J Cancer 1990;62:954–
38. Ying HY, Gong CJ, Feng Y, Jing DD, Lu LG. Serine protease inhibitor Kazal type 1 (SPINK1) downregulates E-cadherin and induces EMT of hepatoma cells to promote hepatocellular carcinoma metastasis via the MEK/ERK signalingpathway.J Dig Dis 2017 Jun; 18 (6):349-358.
39. Higashiyama M, Doi O, Kodama K,Yokouchi H, Tateishi R, Matsuura N, Murata A, Tomita N, Monden T, Ogawa M. Immunohistochemical analysis of pancreatic secretory trypsin inhibitor expression in pulmonary adenocarcinoma: its possible participation in scar formation of the tumor tissues. Tumour Biol 1992;13:299–
40. Xu L, Lu C, Huang Y, Zhou J, Wang X, Liu C, Chen J, Le H. SPINK1 promotes cell growth and metastasis of lung adenocarcinoma and acts as a novel prognostic biomarker. BMB Rep 2018; 51(12):648-653.
41. Tomlins SA, Rhodes DR, Yu J,Varambally S, Mehra R, Perner S, Demichelis F, Helgeson BE, Laxman B, Morris DS, Cao Q, Cao X, Andrén O, Fall K, Johnson L, Wei JT, Shah RB, Al-Ahmadie H, Eastham JA, Eggener SE, Fine SW, Hotakainen K, Stenman UH, Tsodikov A, Gerald WL, Lilja H, Reuter

VE, Kantoff PW, Scardino PT, Rubin MA, Bjartell AS, Chinnaiyan AM. The role of SPINK1 in ETS rearrangement negative prostate cancers. Cancer Cell 2008;13:519–

42. Lee YC, Pan HW, Peng SY, Lai PL, Kuo WS, Ou YH, Hsu HC. Overexpression of tumour-associated trypsin inhibitor (TATI) enhances tumour growth and is associated with portal vein invasion, early recurrence and a stage-independent prognosticfactor of hepatocellular carcinoma. Eur J Cancer 2007 Mar;43(4):736-44.
43. Räsänen K, Itkonen O, Koistinen H, Stenman UH. Emerging roles of SPINK1 in cancer. Clin Chem 2016 Mar;62(3):449-57.
44. Kevin J. Barnum,Matthew J. O'Connell. Cell cycle regulation by checkpoints. Methods Mol Biol 2014; 1170: 29–40.
45. ChenJ.The Cell-cycle arrest and apoptotic functions of p53 in tumor initiation and progression. Cold Spring Harb Perspect Med 2016 Mar 1; 6(3):a026104.
46. Lim S1, Kaldis P. Cdks, cyclins and CKIs: roles beyond cell cycle regulation. Development 2013 Aug;140(15):3079-93.
47. Trenti A, Grumati P, Cusinato F, Orso G, Bonaldo P, Trevisi L. Cardiac glycoside ouabain induces autophagic cell death in non-small cell lung cancer cells via a JNK-dependent decrease of Bcl-2.Biochem Pharmacol 2014 May 15;89(2):197-209.
48. Wei Y, Pattingre S, Sinha S, Bassik M, Levine B.JNK1-mediated phosphorylation of Bcl-2 regulates starvation-induced autophagy. Mol Cell 2008 Jun 20;30(6):678-88.
49. Wei Y, Sinha S, Levine B. Dual role of JNK1-mediated phosphorylation of Bcl-2 in autophagy and apoptosis regulation. Autophagy 2008 Oct;4(7):949-51.
50. Ohmuraya M, Hirota M, Araki M, Mizushima N, Matsui M, Mizumoto T, Haruna K, Kume S, Takeya M, Ogawa M, Araki K, Yamamura K. Autophagic cell death of pancreatic acinar cells in serine protease inhibitor Kazal type 3-deficient mice. Gastroenterologyn 2005 Aug;129(2):696-705.
51. Ozaki N1, Ohmuraya M, Hirota M, Ida S, Wang J, Takamori H, Higashiyama S, Baba H, Yamamura K. Serine protease inhibitor Kazal type 1 promotes proliferation of pancreatic cancer cells through the epidermal growth factor receptor. Mol Cancer Res 2009 Sep;7(9):1572-81.

Figures

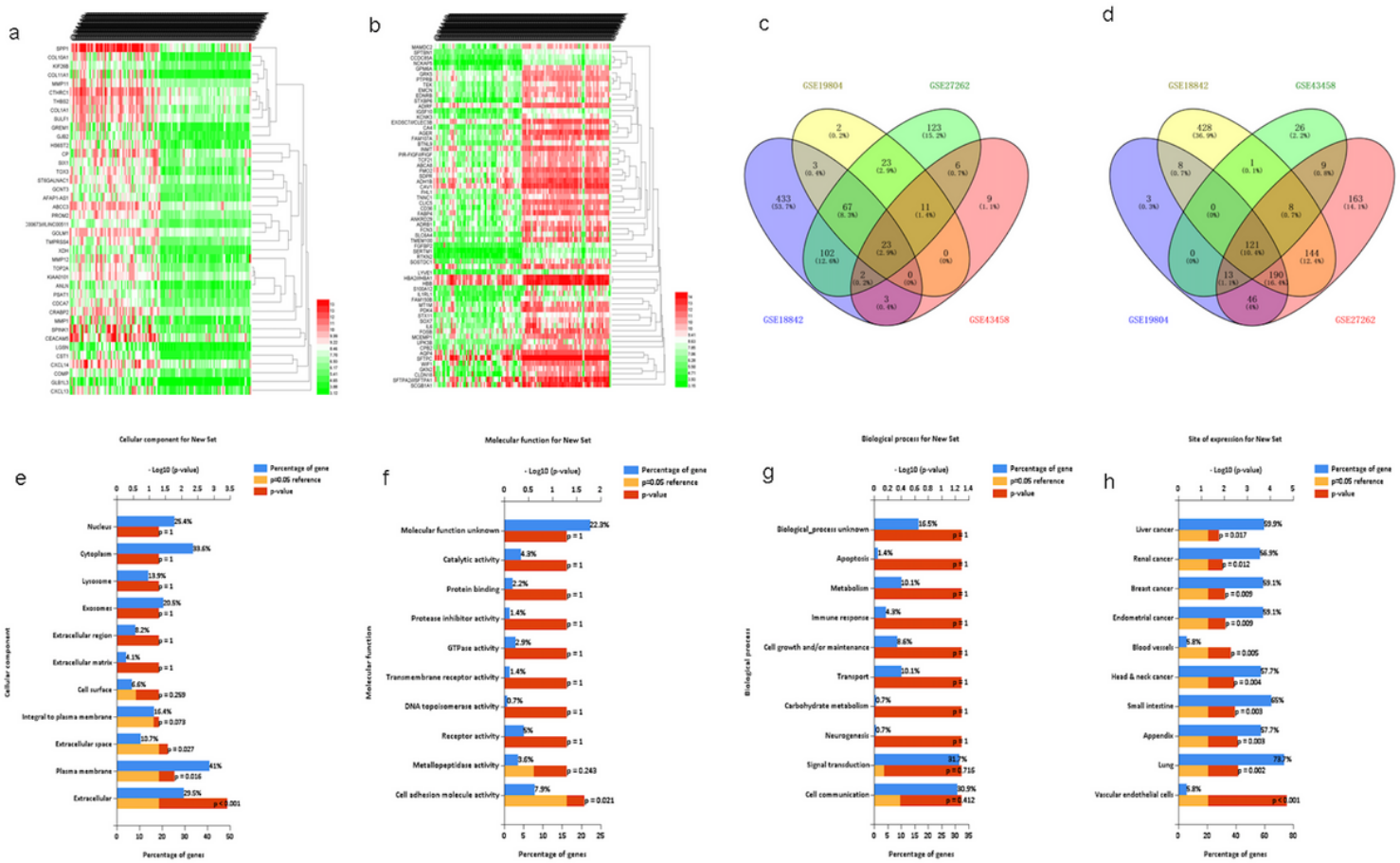


Figure 1

Identification and functional annotation of DEGs. mRNA profiles were downloaded from GSE19804 and analysed by GEO2R. Heapmaps showing (a) up-regulated and (b) down-regulated genes. Venn Diagrams demonstrating (c) up-regulated and (d) down-regulated genes. DEGs were subjected to functional annotation, including (e) cellular components, (f) molecular functions, (g) biological process and (h) sites of expression.

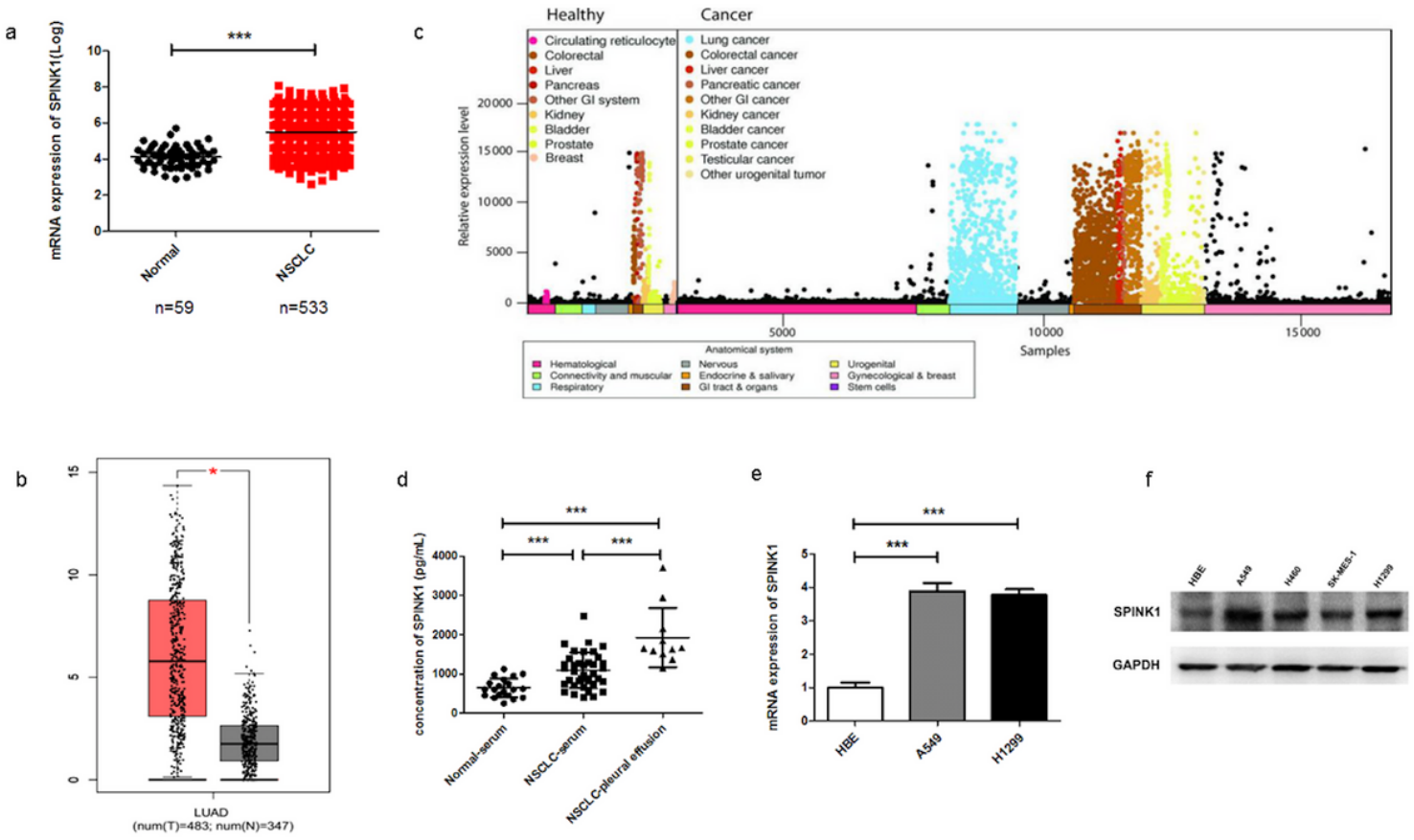


Figure 2

Expression of SPINK1 in NSCLC tissues and cell lines. Expression of SPINK1 in NSCLC tissues in (a) TCGA , (b) GTEx and (c) IST databases. (d) Concentration of SPINK1 detected by ELISA. (e) mRNA and (f) protein levels of SPINK1 in NSCLC cell lines.

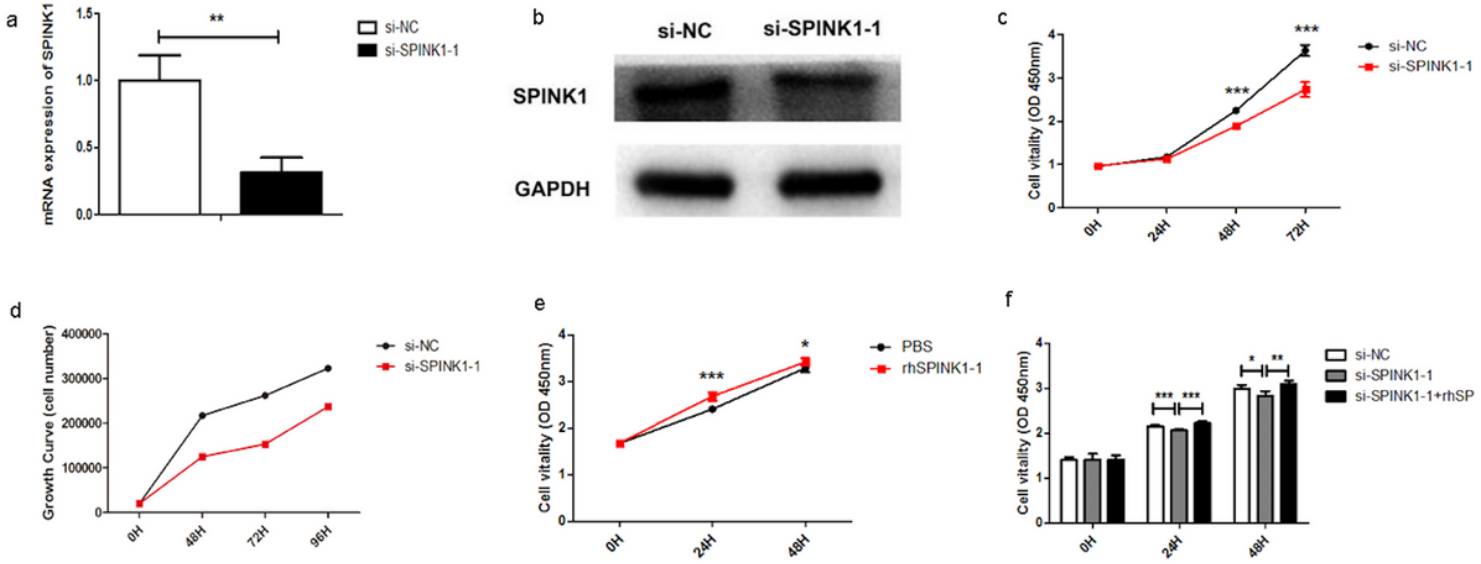


Figure 3

Effect of SPINK1 on proliferation. (a) mRNA and (b) protein expression of SPINK1 in A549 transfected with si-SPINK1-1. (c) Vitality of A549 detected by CCK-8 after knockdown of SPINK1. (d) A549 were transfected with si-SPINK1-1. Number of cells were determined by Neubauer hemocytometer. (e) Vitality of H460 after addition of rhSPINK1 (1ng/mL), detected by CCK-8. (f) rhSPINK1 partially rescued vitality of A549 transfected with si-SPINK1-1.

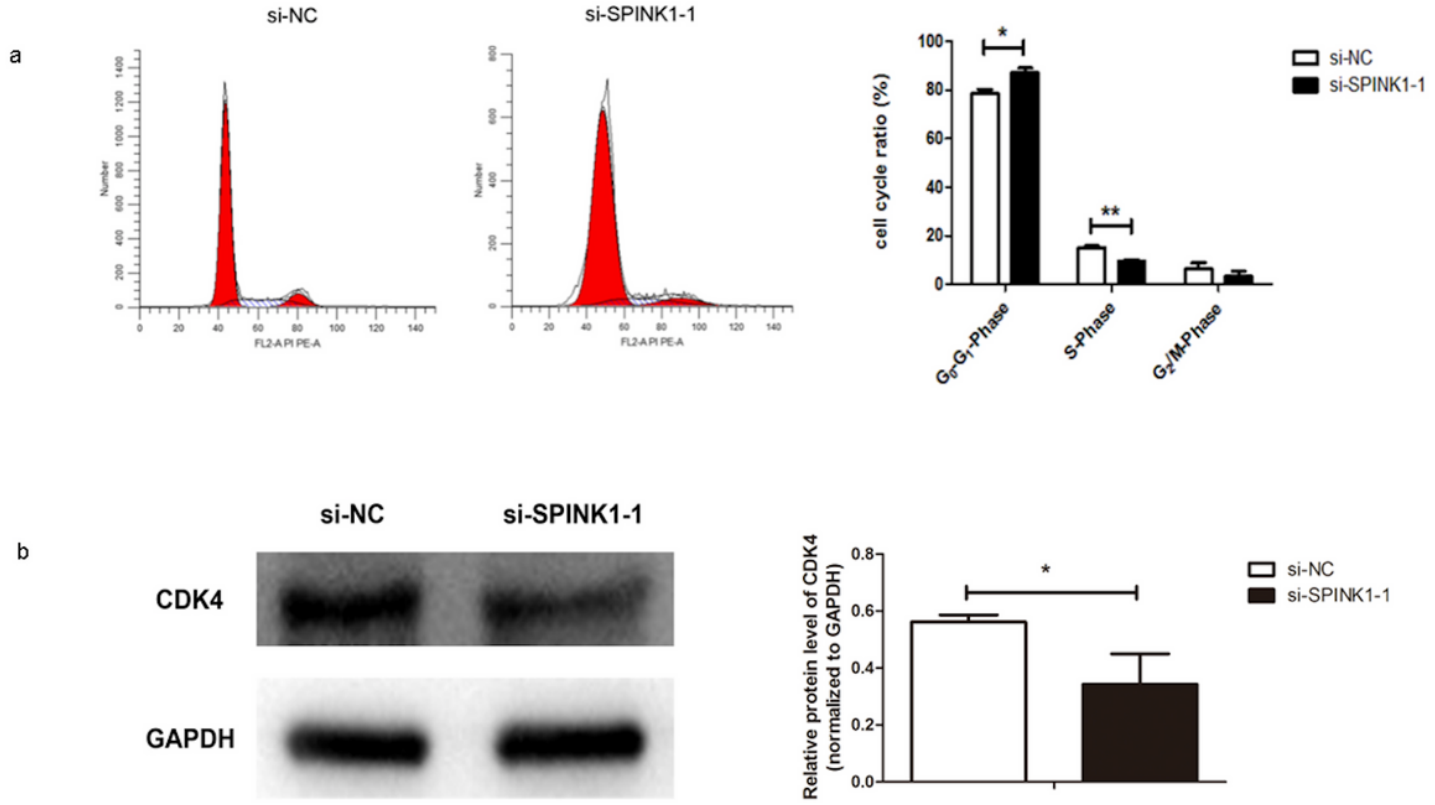


Figure 4

Cell cycle arrest induced by knockdown of SPINK1. (a) Cell cycle distribution was detected by flow cytometry. (b) CDK4 was reduced following treatment with si-SPINK1-1, assessed by WB.

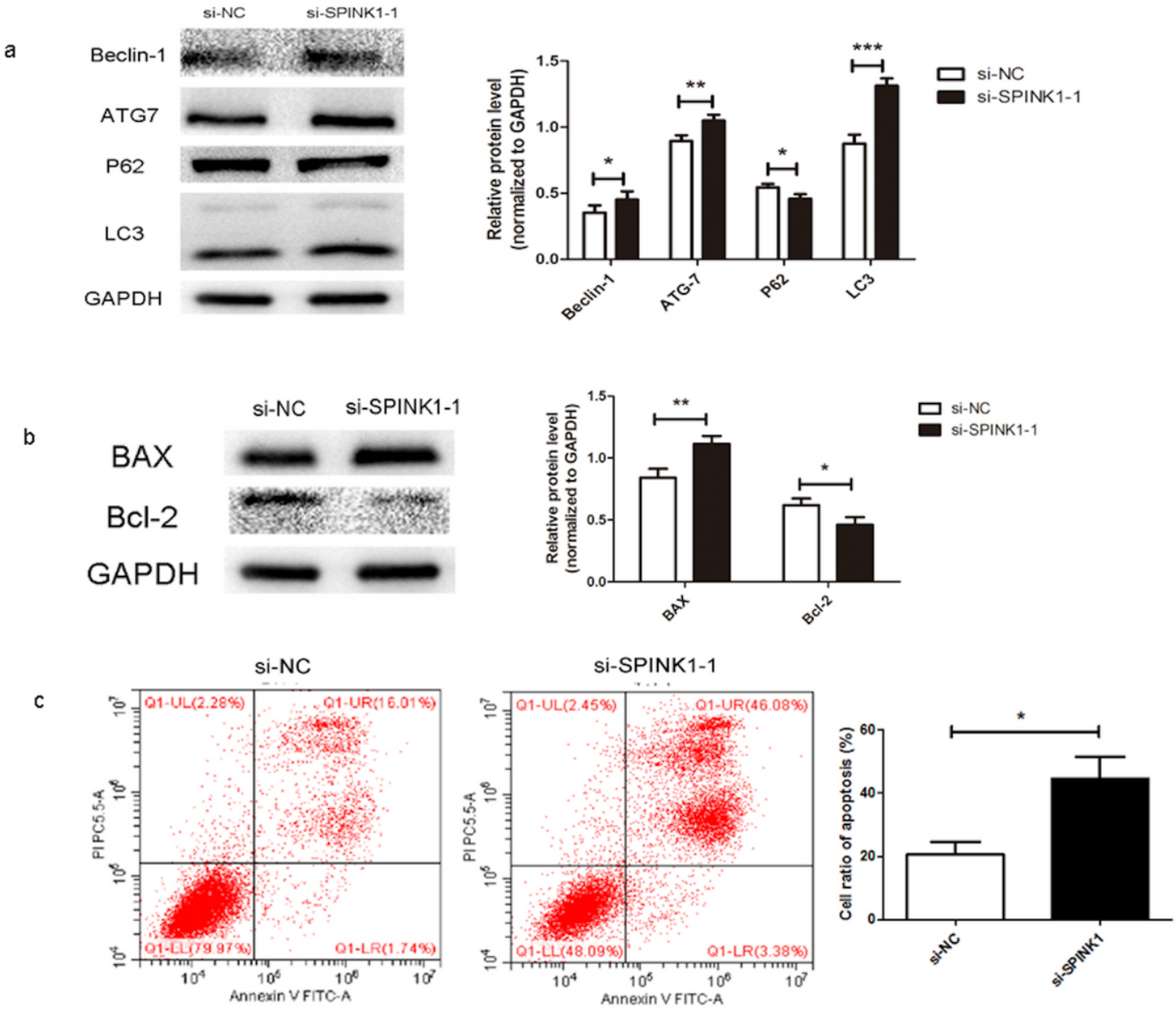


Figure 5

Influence of SPINK1 on autophagy and apoptosis. (a) Activation of autophagy following treatment with si-SPINK1-1, detected by WB. Cell apoptosis was detected by (b) WB and (c) cytometry.

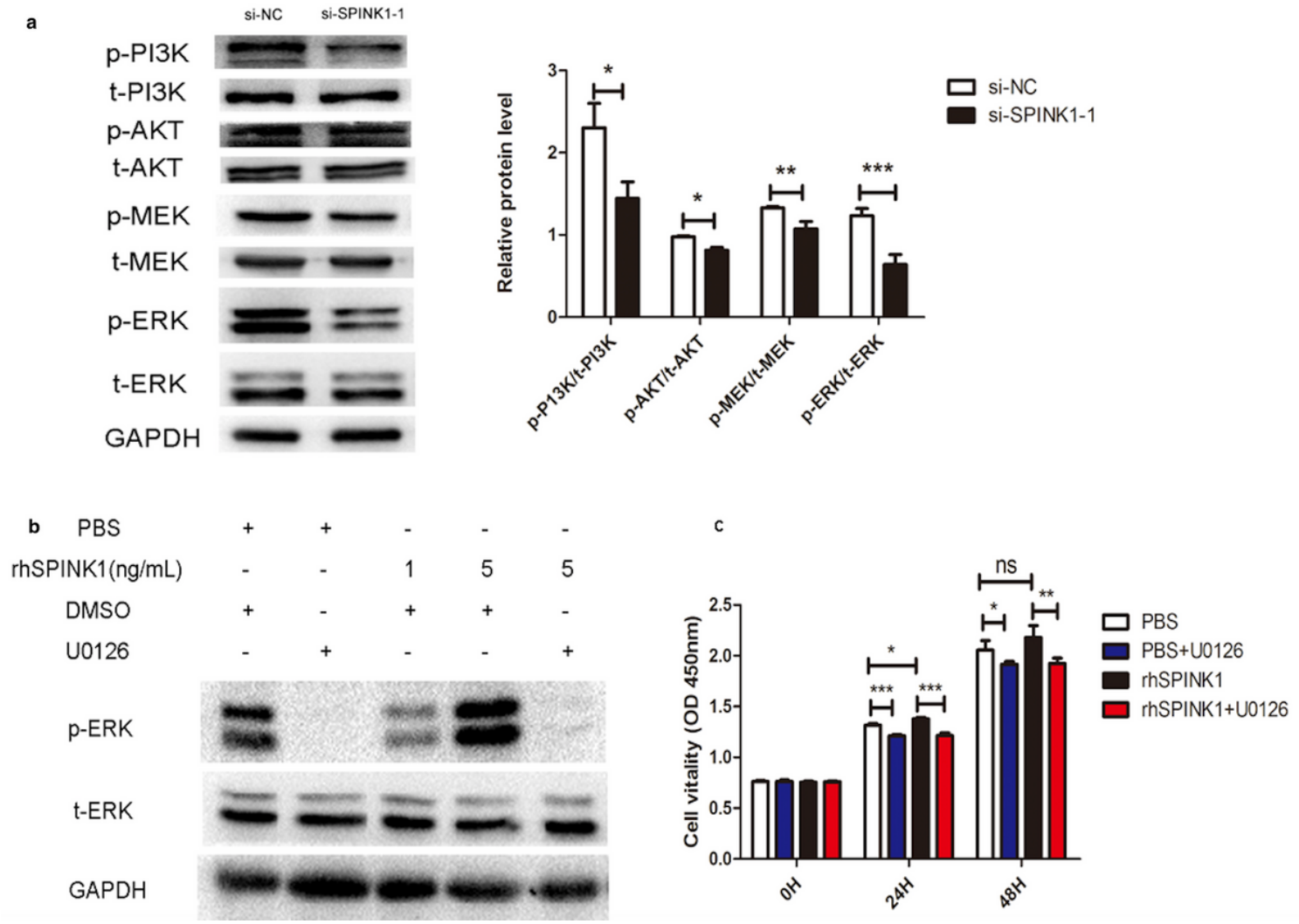


Figure 7

Supplementary Files

This is a list of supplementary files associated with this preprint. Click to download.

- SFig1.doc
- SFig3.doc
- SFig4.doc
- SFig2.doc